Phase Behavior of Polymer-Solvent Mixtures

Dmitry G. Gromov and Juan J. de Pablo*

Department of Chemical Engineering
University of Wisconsin-Madison
1415 Engineering Drive Madison, WI 53706

May 1997

Keywords:

molecular simulation, vapor-liquid equilibria, polymers, supercritical solvents

Abstract

Phase equilibria for mixtures of a polymer and a supercritical solvent are investigated by means of Expanded Gibbs Ensemble simulations. Our results indicate that such systems exhibit both lower and upper critical solution temperature (LCST and UCST) phenomena. Closed-loop miscibility diagrams are observed for systems with no specific preferences for like and unlike components. The results of our simulations for Lennard-Jones polymer-solvent mixtures are in qualitative agreement with experimental data for polymers in supercritical solvents.

Introduction

Solutions of polymers and supercritical fluids (SCF) are encountered in a variety of chemical processes [1, 2]. A substance is said to be supercritical if it is at conditions above its critical temperature T_c and critical pressure P_c. A unique feature of SCFs near the critical point is that their properties (e.g. density) are highly susceptible to small changes of pressure; this increased susceptibility can be used advantageously to achieve desirable processing conditions. For polymers, the quality of a solvent is related to its density. Solvent quality can therefore be fine-tuned by small changes in pressure, thereby providing a means to control solubility. By controlling the solubility of different molecular-weight polymer, it is possible to conceive and design polymer fractionation processes. While several experimental studies have examined the phase behavior of SCF/polymer mixtures (see, for example, [1] and references therein), theoretical work has lagged behind. The complex interplay of density and solvent quality encountered in SCF/polymer mixtures has precluded development of successful theories for these systems. Furthermore, computer simulation studies of phase equilibria for polymers in supercritical solvents have been, to the best of our knowledge, nonexistent.

For polymer systems that exhibit an LCST, polymer solubility decreases with increasing temperature. When both polymer and solvent are highly polar, the LCST is usually below the boiling temperature of the solvent. In contrast, if both components are non-polar, the LCST is usually found at temperatures close to or above the critical temperature of the pure solvent. The so-called LCST behavior has been attributed to a large difference between the thermal expansion coefficient of the polymer and that of the solvent; the latter expands much faster than the former as their mixtures are heated. Adding polymer to the solvent lowers the solvent's density, thereby decreasing the translational entropy of solvent molecules. Eventually, as solvent molecules loose the ability to group around a chain molecule to dissolve it, the polymer precipitates.

A traditional approach to polymer thermodynamics has been provided by the

lattice model of Flory and Huggins [3]. This model gives a simple expression for the free energy of mixing ΔG_{mix} in terms of volume fractions, chain lengths and the Flory interaction parameter χ. The χ parameter was originally intended to reflect a difference in energetic interactions between polymer segments and the solvent. However, in its original formulation, the Flory-Huggins model only predicts UCST behavior and it significantly underestimates the critical solution (or demixing) temperature. The neglect of compressibility effects is responsible for the model's inability to predict the experimentally observed LCST behavior. Furthermore, Flory-Huggins theory predicts that a polymer should be fully soluble in its own monomer ($\chi = 0$) under all conditions. Our results provide exact theoretical evidence that this is not the case and that both LCST and UCST can occur in such nominally athermal systems with simple interactions.

Kiran *et. al.* [1] have studied the effect of molecular weight on the demixing pressure of polystyrene and polyethylene dissolved in supercritical n-alkanes. For low-molecular-weight polystyrene (molecular weight 1,240) in near-critical n-butane, they find LCST-type behavior. However, for molecular weights above 9,000, this systems exhibit UCST-type behavior. The molecular weight was found to significantly influence the minimum pressures required to achieve complete miscibility. In contrast, these authors report that polyethylene (molecular weights 2,100, 16,400, 108,000 and 420,000) in near critical n-pentane exhibits LCST-type behavior. They also show that the maximum in the pressure-concentration coexistence curves shifts to lower polymer concentrations with increasing molecular weight. Chen *et. al* [4] studied the effect of molecular weight on the propylene/poly(ethylene-propylene) demixing pressure in the LCST region. Demixing pressure is highly sensitive to the polymer molecular weight below 30,000. For higher molecular weights, demixing pressure depends on the polymer molecular weight only weakly (if at all). Experimental pressure-temperature boundaries for 1-butene/poly(ethylene-propylene) mixtures [5, 4] and n-pentane/polyethylene [1] indicate that the molecular weight dependence of both

demixing pressure and temperature is more pronounced for low-molecular-weight polymers. These data suggest that an infinite-chain length limit exists for both critical temperatures and pressures.

In this work, we simulate phase equilibria for polymer/SCF systems over a wide range of pressures, temperatures and chain lengths. To the best of our knowledge, aside from a recent letter [6], these results provide the first direct theoretical evidence of the existence of both UCST and LCST for Lennard-Jones polymers dissolved in their own monomer. Even in systems for which there are no specific interactions between like and unlike components, we observe closed miscibility loops. The observed behavior is explained in terms of compressibility and solvent quality. Our simulations have been conducted in the framework of the recently proposed Expanded Gibbs Ensemble [7] using a multiple-time-step hybrid Monte Carlo method [8]. This approach permits direct constant-pressure simulations of phase equilibria for solutions of moderately long chains (e.g. 100 segments).

Simulations

The Gibbs Ensemble Monte Carlo (GEMC) [9] method is widely used for simulations of phase equilibria. Unfortunately, it runs into severe difficulties as the density and size of the molecules increase. This problem can be alleviated to some extent by using a combined Continuous Configurational Bias (CCB)-GEMC [10] method. The Expanded Gibbs Ensemble (EGE) [7] methods employed in this work extends even further the range of chain lengths amenable to simulations of phase equilibria (both VLE and LLE).

One of the major limitations of conventional GEMC resides in the required exchange of molecules between two boxes; for chain molecules, the probability of successful exchanges becomes very small. The conventional algorithm is based on random

insertions of a molecule; CCB methods replace highly unfavorable random trial insertions of large molecules with more favorable biased insertion attempts. The bias is subsequently removed by appropriately modifying the acceptance criteria for molecule transfer attempts.

In the framework of the EGE method, only a few segments of a chain are transferred at a time (as opposed to the whole chain). This results in a significant increase of the acceptance of trial insertions, thereby permitting simulations of longer molecules. The EGE method can be coupled with CCB segmental insertions and deletions of a 'tagged' chain. Since this tagged chain need not be transferred as a whole from one box to the other, parts of it can be present in both boxes at any given time. However, to satisfy conservation of mass, a chain-length increase in one of the boxes is accompanied by an equivalent chain-length decrease in the other box. If a tagged chain reaches its full length or disappears completely, a new tagged chain must be chosen. Thermal equilibration of the system is achieved by means of a multiple-time-step hybrid Monte Carlo method. In this method global updates of the positions of all molecules are attempted at every MC step [8].

Results and Discussion

The polymers studied in this work consist of fully flexible Lennard-Jones chains. Adjacent sites on the chains are connected by stiff springs. The spring potential-energy function is given by $U^{spr}(r) = H(Q_0 - r)^2$, where H is a force constant, and Q_0 is the minimum-energy distance. Throughout this work we have used $H = 1000$ and $Q_0 = \sigma$. These values lead to an average bond length of approximately σ (where σ is the Lennard-Jones size parameter); the resulting chains can be considered to consist of tangent LJ sites. The LJ parameters have been chosen to be $\sigma_{11} = \sigma_{22} = \sigma_{12} = 1.0$, and $\epsilon_{11} = \epsilon_{22} = \epsilon_{12} = 1.0$. The cutoff distance has been set to $r_c = 2.5\sigma$, and the potential has been shifted to ensure continuity at the cutoff. The number of chains used

in our simulations varied from 10 for 64-mers to 20 for 16-mers. The number of solvent molecules was chosen such that the overall composition was inside the coexistence curve. Up to 2000 solvent molecules were necessary for simulations of 64-mers to bring the overall composition into the unstable region. A simulation cycle consisted (per box) of one hybrid MC move (10-20 multiple time step Molecular Dynamics moves in each), three volume moves, and at least 100 transfer moves. A total of at least 1.5×10^4 cycles were used for all runs.

We have characterized the critical properties of the fluid with cut and shifted Lennard-Jones potential [12]. Our estimates for the critical parameters of the solvent (LJ potential, $r_c = 2.5\sigma$, shifted by 0.0163168ϵ so that the potential is exactly zero at cutoff) are in agreement with those reported by Smit [11]

$$T_c^* = 1.085 \pm 0.005, \qquad \rho_c^* = 0.317 \pm 0.006$$

We place the critical point at

$$T_c^* = 1.08, \qquad P_c^* = 0.10, \qquad \rho_c^* = 0.31$$

We use these critical parameters as a frame of reference and report our results in reduced units relative to these values.

We now consider LJ chains dissolved in a supercritical LJ solvent. If the system were incompressible and randomly mixed, the bare Flory interaction parameter $\chi \propto 2\epsilon_{12} - \epsilon_{11} - \epsilon_{22}$ would be exactly zero and, according to Flory-Huggins theory, the polymer would be soluble under any conditions. Limited miscibility is a direct consequence of non-random packing and compressibility effects. For polymeric systems that exhibit an LCST, lower temperatures are required to achieve full miscibility as the chain length is increased (at constant pressure). In Figure (1) coexistence curves are shown for 16, 32, 48 and 64-mers at $P^*/P_c = 2.0$. All polymers investigated here become fully soluble at temperatures below $T^*/T_c \sim 1.13$

Figure (2) presents representative experimental LCST data for poly(ethylene-propylene) in 1-butene [4]. For all pressures reported in the literature, the LCST is highly sensitive to molecular weight below 20,000. For higher molecular weights, the LCST depends only weakly (if at all) on molecular weight. Figure (3) shows simulated LCSTs as a function of chain length; Consistent with experiment, we find that the for low-to-intermediate chain lengths the LCST is highly sensitive to molecular weight. To make a connection between experiment and simulation, we use the notion of an 'equivalent segment' [13]. Equivalent segments consist of a number ($\sim$ 10 for most synthetic polymers) of real repeat units and can be viewed as statistically independent. Stiffer polymer chains have larger numbers of repeat units per equivalent segment. The characteristic ratio C_∞ provides a measure of equivalent segment size. For polyethylene and polypropylene $C_\infty \sim 7$ [13]. Equating a Lennard-Jones bead to an equivalent segment gives a molecular weight of approximately 150 per bead. When we use this number to map our model predictions onto the experimental results (Figure (2)) we find that the lowest experimental polymer molecular weight (790) corresponds to a 5-bead chain. Our longest chain length (64 beads) would be representative of a polymer molecular weight of 9,600. The first two data points in Figure (2) are, therefore, within the range of chain lengths investigated in our simulation.

An important quantity for design of engineering processes is the relative change in the LCST as the polymer molecular weight increases. From Figure (2) we conclude that at $P/P_c = 1.25$, the experimental LCST temperature drops $\sim$ 11.5 percent as the polymer molecular weight changes from 790 to 10,000. After extrapolating the simulation results in Figure (3) to a chain length of 5, we estimate a drop of $\sim$ 10 percent in the LCST as the chain length increases from 5 to 64, which is in good agreement with experiment.

The simulated dependence of the LCST on polymer molecular weight shows signs of leveling off for the upper chain lengths considered in this work. However, the longest chains investigated here are insufficient to draw any additional conclusions regarding

the asymptotic behavior of these systems. Experimentally, the LCST temperature seems to reach a plateau value for relatively high molecular weights (on the order of $\sim 100,000$ for poly(ethylene-propylene) in 1-butene). Our results are in qualitative agreement with experimental pressure-temperature boundaries for 1-butene/poly(ethylene-propylene) [5, 4] and n-pentane/ polyethylene [1], both of which indicate a monotonic decrease of the LCST temperature with polymer molecular weight.

Figure (4) shows temperature-composition diagrams for LJ chains ($N = 16$) in a solvent at two pressures ($P^*/P_c = 2.0$ and $P^*/P_c = 2.4$). A closed immiscibility loop is observed for both pressures. The miscibility gap is substantially broader for the lower pressure, which indicates that, as expected, solvent quality improves with increasing pressure. Figure (5) shows temperature-density coexisting curves for the same system. The densities of the coexisting phases differ substantially; the density of polymer-rich phase is much higher than that of the polymer-lean phase. We can resort to qualitative arguments to construct a physical picture of this nontrivial closed immiscibility loop behavior. Under all conditions, the solvent always has a lower density than the polymer melt. Mixing the two results in a solution with a density intermediate between that of the solvent and that of the polymer. The degree of miscibility will be determined by two opposing forces. A higher solution density is energetically favorable; a large translational entropy, however, is favored by low densities. At temperatures below the LCST, the enthalpic and entropy-of-mixing contributions to ΔG_{mix} are more important than the loss of translational entropy by the solvent; the system therefore prefers to form a one-phase solution. As the temperature increases, the solvent expands very rapidly; the entropy of the solvent rises significantly as the density decreases. Dissolving the polymer would lead to a higher solution density and a corresponding loss of translational entropy. Above the LCST, the penalty for loss of translational entropy by the solvent becomes too large, and the system splits into distinct low-density polymer-lean and high-density polymer-rich phases (Figure 5). As the system temperature increases further, a situation is reached for which enthalpic contributions

dictate the thermodynamic behavior of the mixture. Higher densities are favored by energetic interactions. At some temperature the density of the solvent becomes so low, that the high values of translational entropy are no longer sufficient to maintain a high potential energy of the low-density polymer-lean phase. At this point the system prefers to form a one-phase solution with a density intermediate between that of the pure polymer and the pure solvent.

Conclusions

For the first time, we report from computer simulations the existence of both LCST and UCST in polymer / supercritical monomer systems. The simulations were carried out in the Expanded Gibbs Ensemble in conjunction with the multiple time step Hybrid Monte Carlo technique. This approach allows for direct constant-pressure phase equilibria calculations in polymeric systems consisting of relatively long chains. The simulated phase diagrams take the shape of a closed immiscibility loop. The solvent density and compressibility are the key factors that determine phase equilibria, and we quantify the effects of pressure and temperature on polymer solubility. Lowering the pressure leads to a decrease of polymer solubility and shifts the LCST to lower values. By adjusting the pressure, one can control the width (and the existence) of the miscibility gap and ultimately reach conditions of full miscibility. For the chain lengths investigated in this work (16 - 64) we observe a monotonic decrease of the LCST with chain length. This decrease is consistent with experiment. The simulated and experimental LCSTs suggest that an asymptotic critical temperature (pressure dependent) is reached as the polymer molecule becomes large.

Equation-of-state modeling studies of polymer-near-critical solvent mixtures have consistently failed to accurately predict the phase behavior of such systems (and, in particular, LCST behavior) from knowledge of pure-component properties [1]. The simulation results presented in this work provide a much needed testbed for develop-

ment of improved equations of state capable of predicting the phase behavior of such systems.

Acknowledgments

The authors would like to thank G. Luna-Barcenas, I.C. Sanchez and K.P. Johnston for valuable discussions. This work was supported through a PECASE award from the National Science Foundation. One of the authors (JJdP) is also grateful to the Dreyfus Foundation for a Camille Dreyfus Teacher-Scholar Award.

LIST OF SYMBOLS

$$\begin{aligned}
\Delta G_{mix} &= \text{Gibbs energy of mixing} \\
P^* &= \text{reduced pressure} \\
T^* &= \text{reduced temperature} \\
P_c^* &= \text{solvent critical pressure} \\
T_c^* &= \text{solvent critical temperature} \\
r_c &= \text{cutoff distance} \\
C_\infty &= \text{polymer characteristic ratio}
\end{aligned}$$

Greek letters

$$\begin{aligned}
\chi &= \text{Flory's } \chi \text{ parameter} \\
\epsilon &= \text{energy parameter} \\
\sigma &= \text{size parameter} \\
\rho_c^* &= \text{solvent critical density}
\end{aligned}$$

Subscripts

$$c \quad = \quad \text{critical point}$$

FIGURE CAPTIONS

- **Figure 1:** Demixing temperatures for LJ polymer in LJ solvent at $P^*/P_c^* = 2$ as functions of polymer concentration for various chain lengths N. Circles: $N = 16$, squares: $N = 32$, diamonds: $N = 48$, triangles: $N = 64$. Temperature units are relative to solvent T_c. The line is a guide to the eye.

- **Figure 2:** LCST dependence on the polymer molecular weight for 1-butene / poly(ethylene-propylene) from experimental data [4]. The line is a guide to the eye.

- **Figure 3:** LCST dependence on the polymer chain length from EGE simulations (see also Figure (1)). The line is a guide to the eye.

- **Figure 4:** Demixing temperatures for LJ polymer ($N = 16$) in LJ solvent at $P^*/P_c^* = 2.0$ (circles) and $P^*/P_c^* = 2.4$ (squares) as function of polymer concentration. Temperature units are relative to solvent T_c. The line is a guide to the eye.

- **Figure 5:** Demixing temperatures for LJ polymer ($N = 16$) in LJ solvent at $P^*/P_c^* = 2.0$ (circles) and $P^*/P_c^* = 2.4$ (squares) as function of solution density. Temperature units are relative to solvent T_c. The line is a guide to the eye.

References

[1] E. Kiran. In E. Kiran and J.M.H. Levelt Sengers, editors, *Supercritical Fluids. Fundamentals for Application*. Kluwer Academic Publishers, 1994.

[2] L.A. Kleintjens. In E. Kiran and J.M.H. Levelt Sengers, editors, *Supercritical Fluids. Fundamentals for Application*. Kluwer Academic Publishers, 1994.

[3] P.G. Flory. *Principles of Polymer Chemistry*. Cornell University Press, Ithaca, 1953.

[4] S.J. Chen, I.G. Economou, and M. Radosz. *Macromolecules*, 25:4987, 1992.

[5] S.J. Chen and M. Radosz. *Macromolecules*, 25:3089, 1992.

[6] G. Luna-Bárcenas, D.G. Gromov, J.C. Meredith, I.C. Sanchez, J.J. de Pablo, and K.P. Johnston. *Phys. Rev. Lett., submitted*, 1997.

[7] F. Escobedo and J.J. de Pablo. *J. Chem. Phys.*, 105(10):4391, 1996.

[8] D.G. Gromov and J.J. de Pablo. *J. Chem. Phys.*, 103(18):8247, 1995.

[9] A.Z. Panagiotopoulos, N. Quirke, M. Stapleton, and D.J. Tildesley. *Mol. Phys.*, 63(4):527, 1988.

[10] M. Laso, J.J. de Pablo, and U.W. Suter. *J. Chem. Phys.*, page 2817, 1992.

[11] B. Smit. *J. Chem. Phys.*, 96:8639, 1992.

[12] D.G. Gromov. PhD thesis, Univesity of Wisconsin-Madison, 1997.

[13] P.G. Flory. *Statistical Mechanics of Chain Molecules*. Hanser Publishers, 1989.

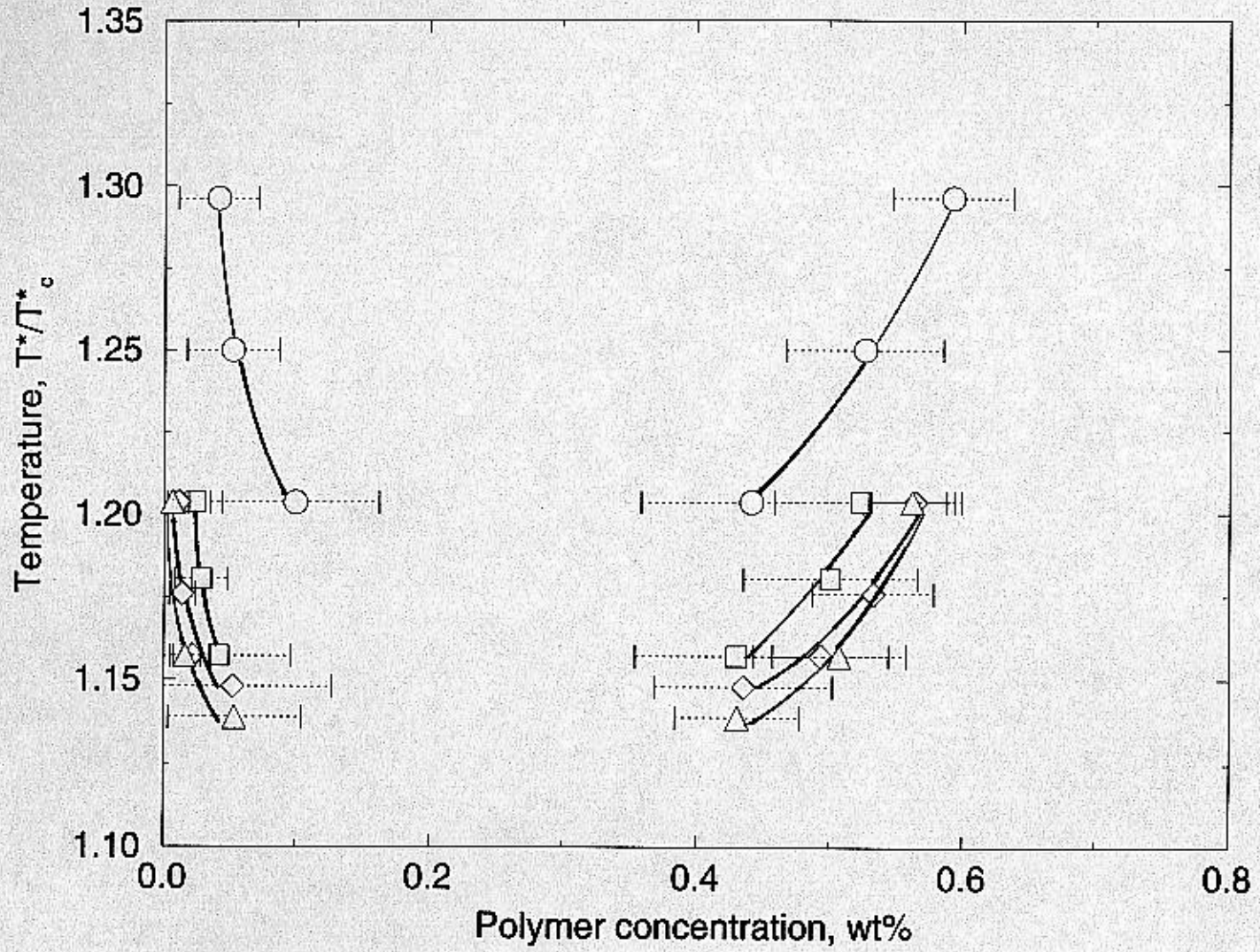
1.35
1.30
1.25
1.20
1.15
1.10
Temperature, T*/T*c
0.0
0.2
0.4
0.6
0.8
Polymer concentration, wt%

fig1 Gromov . . .

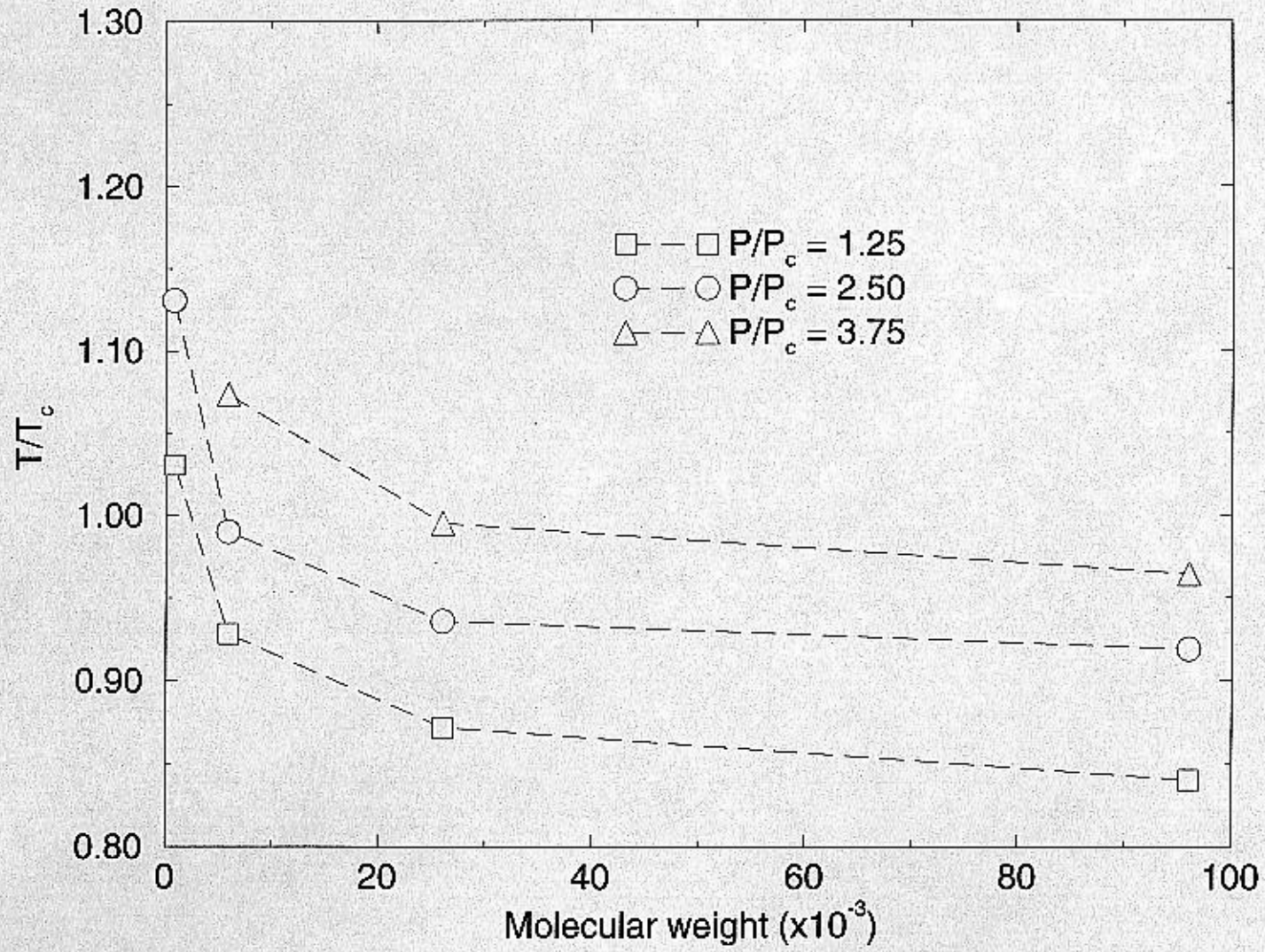
1.30
1.20
1.10
1.00
0.90
0.80
T/T$_c$
0
20
40
60
80
100
Molecular weight (x10^{-3})
P/P$_c$ = 1.25
P/P$_c$ = 2.50
P/P$_c$ = 3.75

fig 2 Gromov . . .

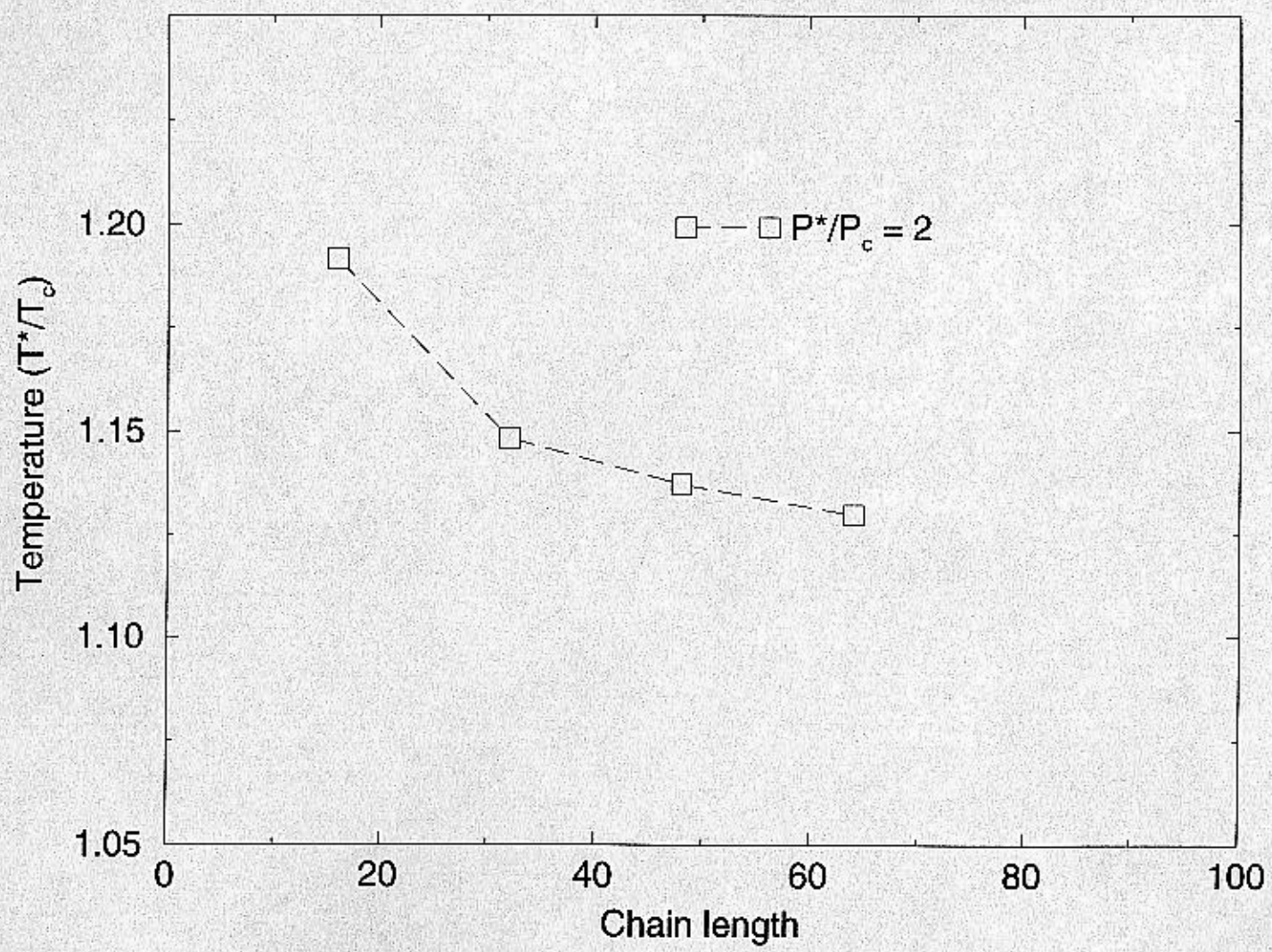
P*/P_c = 2
Temperature (T*/T_c)
1.20
1.15
1.10
1.05
0
20
40
60
80
100
Chain length

fig 3 Gromov . . .

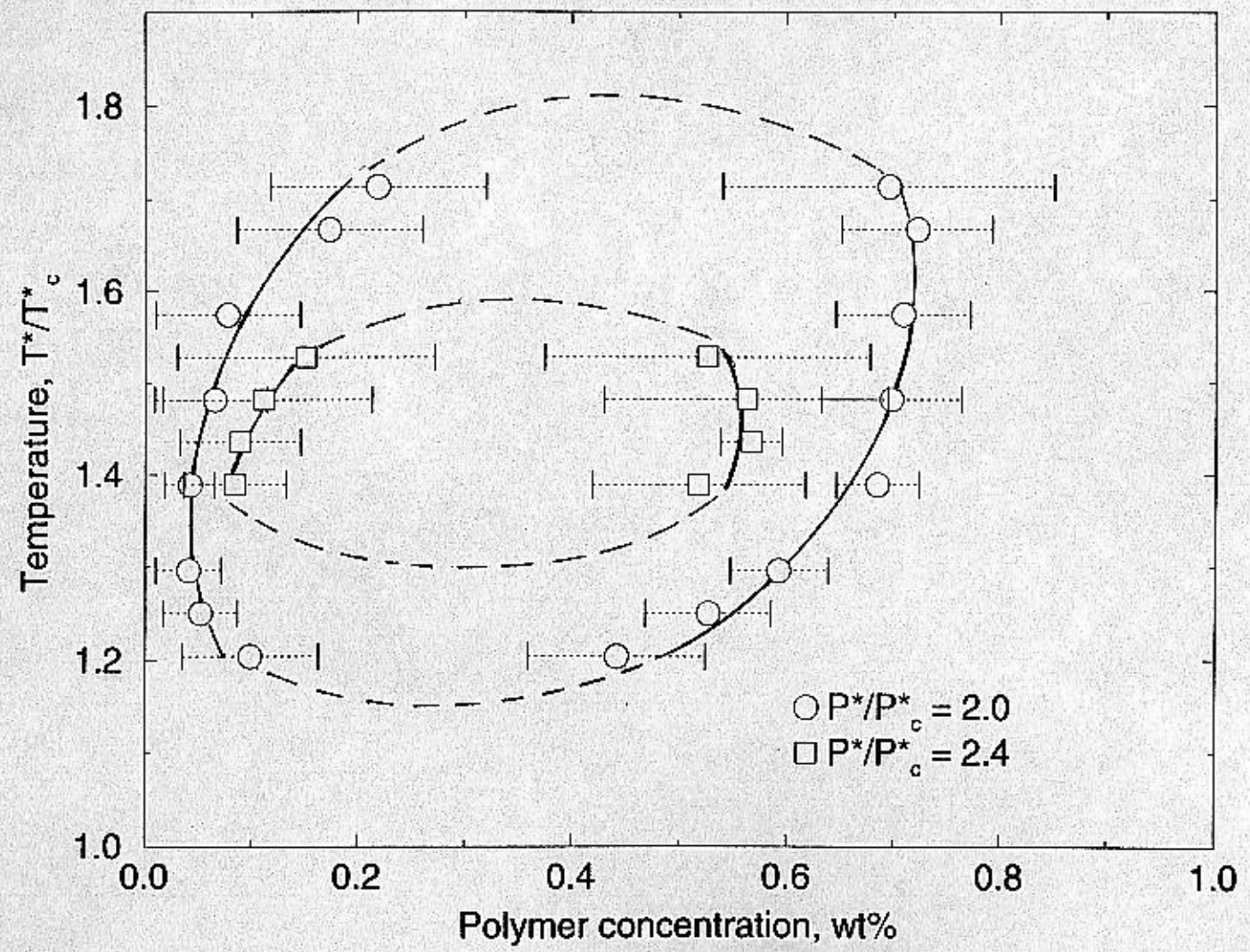
1.8
1.6
1.4
1.2
1.0
Temperature, T*/T*c
0.0
0.2
0.4
0.6
0.8
1.0
Polymer concentration, wt%
P*/P*c = 2.0
P*/P*c = 2.4

fig 4 Gromov . . . .

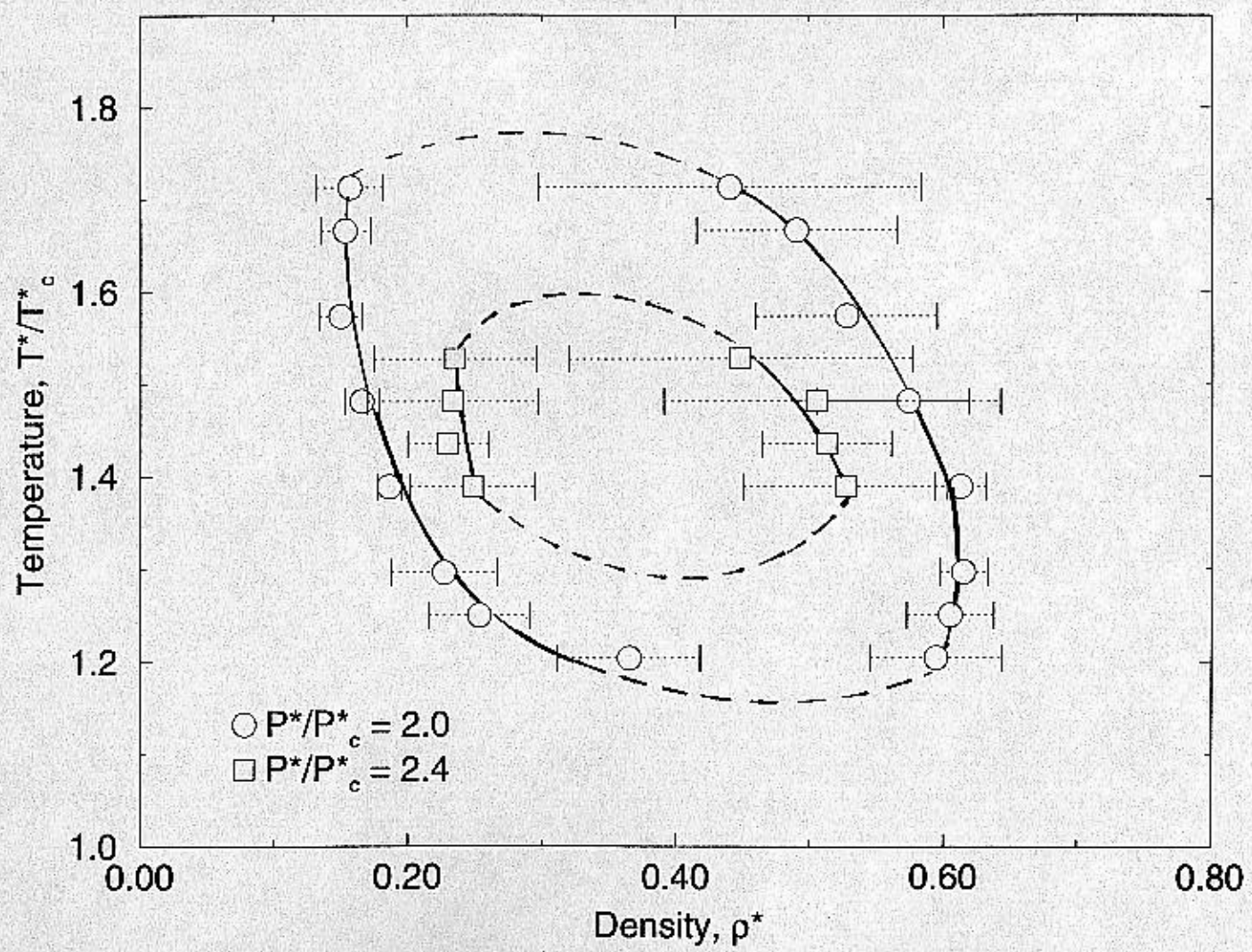
1.8
1.6
1.4
1.2
1.0
Temperature, T*/T*c
0.00
0.20
0.40
0.60
0.80
Density, ρ*
P*/P*c = 2.0
P*/P*c = 2.4

fig 5 Gromov . . . .